Qubit Measurements with a Double-Dot Detector

T. Gilad and S. A. Gurvitz

Department of Particle Physics, Weizmann Institute of Science, Rehovot 76100, Israel

(Received 14 June 2006; published 14 September 2006)

We propose to monitor a qubit with a double-dot (DD) resonant-tunneling detector, which can operate at higher temperatures than a single-dot detector. In order to assess the effectiveness of this device, we derive rate equations for the density matrix of the entire system. We show that the signal-to-noise ratio can be greatly improved by a proper choice of the parameters and location of the detector. We demonstrate that quantum interference effects within the DD detector play an important role in the measurement. Surprisingly, these effects produce a systematic measurement error, even when the entire system is in a stationary state.

DOI: 10.1103/PhysRevLett.97.116806 PACS numbers: 73.50.−h, 03.65.Yz, 73.23.−b

The single electron transistor (SET) is a sensitive device for quantum measurements [1–3]. It can be used as a monitor of a charge qubit, provided that the energy level E_0 carrying the current is close to the Fermi levels of the reservoirs $\mu_{L,R}$ [see Fig. 1(a) and 1(a′)]. Then, because of the electrostatic repulsion U between the electrons, the SET current I drops when the qubit is in the state E_2, as in Fig. 1(a′).

It is clear that one needs very low reservoir temperatures in order to use the SET as a sensitive detector. This requirement can be weakened by taking a double dot (DD) for monitoring the qubit state, Fig. 1(b) and 1(b′). In contrast with the SET temperature (T) of the reservoir will not affect the current if $\mu_L - T \gg E_0 \gg \mu_R + T$ [4,5].

Because of quantum interference effects, the dynamics of the measurement process using the DD detector is more complicated than with the SET detector. An electron flowing through the DD can be trapped in a linear superposition of the dot states. As a result, quantum interference could modify the signal in such a way that the DD cannot monitor the qubit. It is necessary to analyze the influence of the DD on the qubit motion (and vice versa) in order to establish the optimal conditions for utilizing the DD as an effective quantum detector. This can be done by solving the Schrödinger equation describing the combined system of qubit and detector.

In fact, the setup shown in Fig. 1(b) and 1(b′) represents a generic class of nondemolition quantum measurements where a measured system interacts with only one state of the apparatus, while the apparatus may be in a superposition of states. This can take place in many devices based on interference, for instance in an electronic Mach-Zehnder interferometer [8,9]. We therefore believe that our analysis of a qubit interacting with the DD detector can be useful for many different quantum measurements.

Let us describe the entire setup shown in Fig. 1(b) and 1(b′) by the tunneling Hamiltonian $H = H_q + H_{dd} + H_{\rm int}$, where

$$
\begin{aligned}
H_q &= E_1 a_1^\dagger a_1 + E_2 a_2^\dagger a_2 + \Omega(a_1^\dagger a_2 + a_2^\dagger a_1),\\
H_{dd} &= H_0 + E_0(c_1^\dagger c_1 + c_2^\dagger c_2) + \gamma(c_1^\dagger c_2 + c_2^\dagger c_1)\\
&\quad + \sum_\lambda (\Omega_\lambda^L c_1^\dagger c_\lambda^L + \Omega_\lambda^R c_2^\dagger c_\lambda^R + \text{H.c.})\\
&\quad + \bar{U}_{12} c_1^\dagger c_1 c_2^\dagger c_2,\\
H_{\rm int} &= U a_2^\dagger a_2 c_2^\dagger c_2
\end{aligned}
\qquad (1)
$$

are the qubit and the DD Hamiltonians, and $H_{\rm int}$ is their interaction. Here $a^\dagger(a)$ is the creation (annihilation) operator for the electron in the qubit and $c^\dagger(c)$ is the same operator for the DD; Ω is the coupling between the states $|a_{1,2}^\dagger|0\rangle$ of the qubit, and γ is the coupling between the states $|c_{1,2}^\dagger|0\rangle$ of the DD. The Hamiltonian $H_0 = \sum_\lambda [E_\lambda^L (c_\lambda^L)^\dagger c_\lambda^L + E_\lambda^R (c_\lambda^R)^\dagger c_\lambda^R]$ describes the reservoirs, where $\Omega_\lambda^{L,R}$ are the couplings between the right and left dots with the right and left reservoirs. We assume weak energy dependence of these couplings, $\Omega_\lambda^{L,R} \simeq \Omega_{L,R}$. Then the corresponding tunneling rates are $\Gamma_{L,R} = 2\pi\rho_{L,R}\Omega_{L,R}^2$, where $\rho_{L,R}$ are the density of states in the reservoirs. The

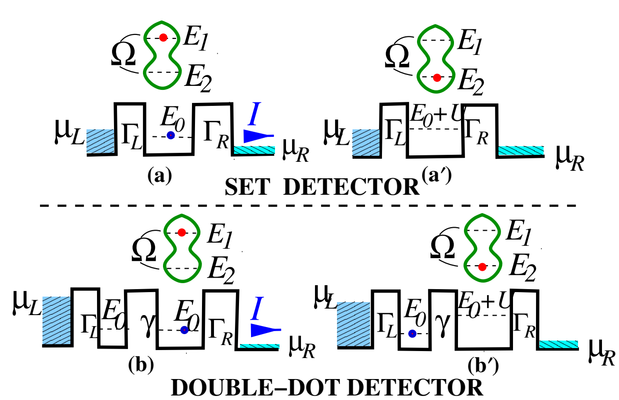

FIG. 1 (color online). The qubit measurements using the SET detector (a),(a′) and the DD detector (b),(b′). $\Gamma_{L,R}$ and γ denote tunneling rates to the reservoirs and the interdot coupling.

latter quantities are also weakly dependent of energy. The last term in H_{dd} describes the interdot repulsion. For simplicity we consider electrons as spinless fermions.

Using the technique developed in Refs. [10,11] for the case of large bias voltage, $V = \mu_L - \mu_R$, we can partially trace out the reservoir states in the equation of motion for the density matrix of an entire system, $i\dot{\varrho} = [H, \varrho]$. As a result we arrive at the Bloch-type rate equations for the reduced density matrix, $\sigma_{ij}^n(t)$, describing the qubit-detector evolution, where the indices i, j denote all available discrete states of the detector-qubit system and n denotes the number of electrons which have arrived at the right reservoir by time t. In our case, Fig. 1(b) and 1(b′), the available discrete states are labeled (a, b, c, d), denoting the cases that the DD is empty (a), the left dot of the DD system is occupied (b), the right dot of the DD system is occupied (c), and both dots are occupied (d), while the electron of the qubit occupies the level E_1 [see Fig. 1(b)]. Correspondingly, (a', b', c', d') denote the same states but where the electron of the qubit occupies the level E_2 [see Fig. 1(b′)]. If the interdot repulsion is large, $\bar{U}_{12} \gg V$, the states d, d' do not contribute terms to the equations of motion. We obtain in this case [10–12]

$$\dot{\sigma}_{aa}^n = -\Gamma_L\sigma_{aa}^n + \Gamma_R\sigma_{cc}^{n-1} + i\Omega(\sigma_{aa'}^n - \sigma_{a'a}^n), \tag{2a}$$

$$\dot{\sigma}_{a'a'}^n = -\Gamma_L\sigma_{a'a'}^n + \Gamma_R\sigma_{c'c'}^{n-1} + i\Omega(\sigma_{a'a}^n - \sigma_{aa'}^n), \tag{2b}$$

$$\dot{\sigma}_{bb}^n = \Gamma_L\sigma_{aa}^n + i\Omega(\sigma_{bb'}^n - \sigma_{b'b}^n) + i\gamma(\sigma_{bc}^n - \sigma_{cb}^n), \tag{2c}$$

$$\dot{\sigma}_{b'b'}^n = \Gamma_L\sigma_{a'a'}^n + i\Omega(\sigma_{b'b}^n - \sigma_{bb'}^n) + i\gamma(\sigma_{b'c'}^n - \sigma_{c'b'}^n), \tag{2d}$$

$$\dot{\sigma}_{cc}^n = -\Gamma_R\sigma_{cc}^n + i\Omega(\sigma_{cc'}^n - \sigma_{c'c}^n) + i\gamma(\sigma_{cb}^n - \sigma_{bc}^n), \tag{2e}$$

$$\dot{\sigma}_{c'c'}^n = -\Gamma_R\sigma_{c'c'}^n + i\Omega(\sigma_{c'c}^n - \sigma_{cc'}^n) + i\gamma(\sigma_{c'b'}^n - \sigma_{b'c'}^n), \tag{2f}$$

$$\dot{\sigma}_{aa'}^n = i\Omega(\sigma_{aa}^n - \sigma_{a'a'}^n) - \Gamma_L\sigma_{aa'}^n + \Gamma_R\sigma_{cc'}^{n-1}, \tag{2g}$$

$$\dot{\sigma}_{bb'}^n = i\Omega(\sigma_{bb}^n - \sigma_{b'b'}^n) + i\gamma(\sigma_{bc'}^n - \sigma_{cb'}^n) + \Gamma_L\sigma_{aa'}^n, \tag{2h}$$

$$\dot{\sigma}_{bc}^n = i\Omega(\sigma_{bc'}^n - \sigma_{b'c}^n) + i\gamma(\sigma_{bb}^n - \sigma_{cc}^n) - \frac{\Gamma_R}{2}\sigma_{bc}^n, \tag{2i}$$

$$\dot{\sigma}_{b'c'}^n = iU\sigma_{b'c'}^n + i\Omega(\sigma_{b'c}^n - \sigma_{bc'}^n) + i\gamma(\sigma_{b'b'}^n - \sigma_{c'c'}^n) - \frac{\Gamma_R}{2}\sigma_{b'c'}^n, \tag{2j}$$

$$\dot{\sigma}_{cc'}^n = iU\sigma_{cc'}^n + i\Omega(\sigma_{cc}^n - \sigma_{c'c'}^n) + i\gamma(\sigma_{cb'}^n - \sigma_{bc'}^n) - \Gamma_R\sigma_{cc'}^n, \tag{2k}$$

$$\dot{\sigma}_{bc'}^n = iU\sigma_{bc'}^n + i\Omega(\sigma_{bc}^n - \sigma_{b'c'}^n) + i\gamma(\sigma_{bb'}^n - \sigma_{cc'}^n) - \frac{\Gamma_R}{2}\sigma_{bc'}^n, \tag{2l}$$

$$\dot{\sigma}_{cb'}^n = i\Omega(\sigma_{cb}^n - \sigma_{c'b'}^n) + i\gamma(\sigma_{cc'}^n - \sigma_{bb'}^n) - \frac{\Gamma_R}{2}\sigma_{cb'}^n. \tag{2m}$$

Note that these equations are obtained from the original many-body equations $i\dot{\varrho} = [H, \varrho]$ without the explicit use of any Markov-type or weak-coupling approximations in the case of large bias voltage, $V \gg \Gamma_{L,R}, U$ [10,11]. There are no other limitations on U, in contrast with our analysis of the SET detector [12].

Equations (2) are different from the standard master equations, describing a quantum system interacting with the environment (detector) by keeping track of the environment variables. In our case this is the number of electrons (n) arriving at the collector. This allows us to find the time evolution of the qubit and the detector at once. For instance, the qubit behavior is described by the (reduced) density matrix $\sigma_q(t) \equiv \{\sigma_{\alpha\beta}(t)\}$ with $\alpha, \beta = \{1, 2\}$, where $\sigma_{11} = \sum_n(\sigma_{aa}^n + \sigma_{bb}^n + \sigma_{cc}^n)$, $\sigma_{12} = \sum_n(\sigma_{aa'}^n + \sigma_{bb'}^n + \sigma_{cc'}^n)$ and $\sigma_{22} = 1 - \sigma_{11}$.

On the other hand, by tracing out the qubit variables we obtain the probability of finding n electrons which have arrived at the collector, $P_n(t) = \sum_j \sigma_{jj}^n(t)$. This quantity allows us to determine the average detector current and its shot-noise spectrum. The former is given by

$$I(t) = e\sum_n n\dot{P}_n(t) = e\Gamma_R\sigma_R(t), \tag{3}$$

where $\sigma_R(t) = \sum_n[\sigma_{cc}^n(t) + \sigma_{c'c'}^n(t)]$ is the probability that the right dot is occupied. The shot-noise spectrum, $S(\omega)$, is obtained from the McDonald formula [13,14]

$$S(\omega) = 2e^2\omega\int_0^\infty dt\sin(\omega t)\sum_n n^2\dot{P}_n(t), \tag{4}$$

One finds from Eqs. (2) and (4) that

$$S(\omega) = 2e^2\omega\Gamma_R\text{Im}[Z_{cc}(\omega) + Z_{c'c'}(\omega)], \tag{5}$$

where $Z_{ij}(\omega) = \int_0^\infty \sum_n(2n+1)\sigma_{ij}^n(t)\exp(i\omega t)dt$. These quantities are obtained directly from Eqs. (2) after the corresponding integration over t [15].

Consider first the static qubit, $\Omega = 0$. Solving Eqs. (2) for this case one finds that the stationary current, $\bar{I} = I(t\to\infty)$ obtains the value $\bar{I}_1 = \Gamma_R\bar{\sigma}_R(U=0)$ when the qubit is in the state E_1, and $\bar{I}_2 = \Gamma_R\bar{\sigma}_R(U)$ when the qubit is in the state E_2, Fig. 1(b) and 1(b′), where

$$\bar{\sigma}_R(U) = \frac{\gamma^2}{U^2 + \frac{\Gamma_R^2}{4} + \gamma^2(2 + \frac{\Gamma_R}{\Gamma_L})}. \quad (6)$$

As expected, the detector current decreases whenever the electron of the qubit is close to the DD detector. Consider now $\Omega \neq 0$. We assume that for an "ideal" detector its average current would follow the qubit motion [16],

$$I(t) = \bar{I}_1\sigma_{11}(t) + \bar{I}_2[1 - \sigma_{11}(t)]. \quad (7)$$

This condition, however, cannot be fully met since the detector's response is limited by the rate of tunneling from the right dot to the collector. Nevertheless, if this transition is fast enough compared to the qubit frequency, $\Gamma_R \gg \Omega$, one expects to approach Eq. (7).

Let us compare $\sigma_{11}(t)$ with the average "signal," $[I(t) - \bar{I}_2]/\Delta\bar{I}$, where $\Delta\bar{I} = \bar{I}_1 - \bar{I}_2$. The results of our calculations for $\gamma = \Omega$ are presented in Fig. 2. The initial conditions correspond to the qubit electron in the upper dot and the detector current $I(t = 0) = \bar{I}_1$. One finds that the detector does not follow the qubit oscillations well when $\Gamma_R = \gamma$, Fig. 2(a). On the other hand, in Fig. 2(b) where $\Gamma_R \gg \gamma$, the detector performance is much improved, in accordance with our arguments.

Yet, the results displayed in Fig. 2(a) are surprising. One expects that in the steady-state limit $(t \to \infty)$ the average detector current should be distributed between the values $\bar{I}_1$ and $\bar{I}_2$, with probabilities σ_{11} and $1 - \sigma_{11}$ to find the qubit in the states $E_{1,2}$, respectively. Equation (7) should thus always hold in the limit of $t \to \infty$ for any such device (for instance, the SET detector [12]). In the case of the DD detector, however, Eq. (7) does not hold in the steady-state limit, as seen in Fig. 2(a). In fact, this can be obtained analytically in the limit of small U by expanding the stationary current, $\bar{I} = I(t \to \infty)$, Eq. (3), in powers of U. One finds for the detector's signal:

$$\frac{\bar{I} - \bar{I}_2}{\Delta\bar{I}} = \left[1 + \frac{2}{4 + (\Gamma_R/2\Omega)^2} + O(U^2)\right]\sigma_{11}(t \to \infty). \quad (8)$$

It follows from this expression that a mismatch between the signal and the qubit (σ_{11}) survives even in the limit $U \to 0$. In this case it depends only on the ratio Γ_R/Ω. The other detector parameters γ and Γ_L enter only in the term proportional to U^2.

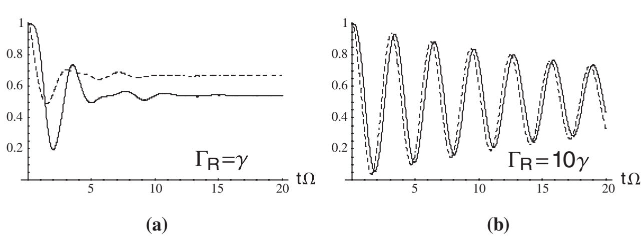

FIG. 2. The probability of finding the qubit in the state E_1, (dashed line) compared with the average detector signal, $[I(t) - \bar{I}_2]/\Delta\bar{I}$ (solid line) for $\gamma = \Omega$ and $U = 5\ \Omega$, $\Gamma_L = 5\ \Omega$.

So where is the "hidden" probability that is responsible for the systematic error in the qubit measurements? It can be recovered in the linear superposition of the detector and qubit states. The DD current flows via two discrete energy levels, E_0 and $E_0 + U$. A carrier wave function thus proceeds through a linear superposition of these states, $b(b')$ and $c(c')$. The qubit is itself a two level system described by superposition. These different superpositions involve the same states (b, b', c, c') of the entire system, and hence are entangled. This is reflected in the off-diagonal terms $\sigma_{bc'}$ and $\sigma_{b'c}$, Eqs. (2). As a result the superposition of qubit states (qubit's "phase") affects the DD dynamics, leading to a violation of Eq. (7). This happens even in the limit $U \to \infty$. In this case the state (c') disappears from Eqs. (2), but the off-diagonal term $\sigma_{cb'}$ still survives in the limit $t \to \infty$. One should note that in the case of the SET such entanglement cannot occur. Therefore Eq. (7) holds for the SET, even though $\sigma_{12}(t \to \infty) \neq 0$.

We find from Fig. 2 and Eq. (7) that the detector's performance improves when $\Gamma_R \gg \Omega$. At the same time, however, its average signal decreases. In order to assess the detector's efficiency this signal should be compared with its noise. An appropriate measure of the detector efficiency is the integrated signal-to-noise ratio [2,19], $s/n = \int_{-\infty}^{\infty}[|I_{\rm sig}(\omega)|^2/S(\omega)]d\omega/2\pi$. The signal $I_{\rm sig}(\omega) = \int_0^{\infty}[I(t) - I(t \to \infty)]\exp(i\omega t)dt$ corresponds to a deviation of the detector current from its stationary value, and can be evaluated using Eqs. (2), (3), and (5). We show in Fig. 3 how the integrated signal-to-noise ratio behaves as a function of both U and the ratio Γ_R/γ, for $\Gamma_L = 5\ \Omega$ and $\gamma = \Omega$. A peak is observed uniformly throughout the range of U at $\gamma \approx 0.4\Gamma_R$. The signal-to-noise ratio depends weakly on U when $U/\Omega \gtrsim 15$, allowing good operation even at low values of U. Comparing the performances of the DD and the SET detectors, we see that the maximal signal-to-noise ratios obtained are comparable. However, the SET reaches these values only in the asymmetric limit $\Gamma_R \gg \Gamma_L$ [12], while the DD detector's signal-to-noise ratio is shown to be optimized without such a restriction.

The results so far presented refer to a qubit that is positioned near the right dot of the detector. One may ask what happens when the qubit is positioned near the left dot. It was suggested in Refs. [12,20] that the performance of any quantum detector would improve if the detector were to operate mostly in the states where there is no actual interaction with the qubit. By this argument one can expect that putting the qubit near the left dot would lead to poor performance. Indeed, in this case the misalignment of the energy levels prevents electron propagation to the right dot, so that the electron is pinned to the left dot. This increases the weight of states where the detector interacts with the qubit. On the other hand, if the qubit is located near the right dot as in Fig. 1(b) and 1(b′), the same misalignment of levels localizes the electron in the left dot, diminishing the occupation of the right dot, Eq. (6). As a result, the actual interaction with the detector decreases and so it is expected to operate better.

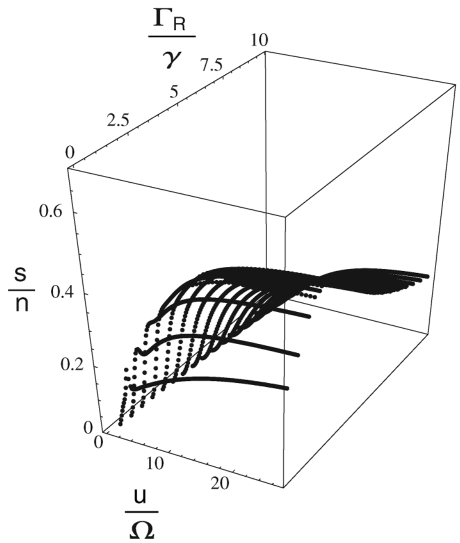

FIG. 3. The integrated signal-to-noise ratio of the DD detector. Here $\gamma = \Omega$, $\Gamma_L = 5\ \Omega$.

Our conclusion about the asymmetry with respect to the qubit's location can be confirmed by direct evaluation of the detector efficiency, in the same way as presented in Figs. 2 and 3. We can also confirm it by evaluating the power spectrum of the detector current, $S(\omega)$, via Eq. (5). This displays a pronounced peak at $\omega = 2\ \Omega$, generated by the qubit oscillations. It was argued in Ref. [18] that the peak-to-background ratio, $S(2\Omega)/S(\omega \to \infty)$, is a measure of the detector efficiency. Figure 4 exhibits this ratio for the two qubit positions as a function of U. As we increase U (the misalignment of the levels) we find that the two curves separate. Thus, the setup with the qubit near the right dot is more effective, in accordance with our arguments. Note that the peak-to-background ratio for this setup depends weakly on U for $U/\Omega \gtrsim 15$. We have already noted that the signal-to-noise ratio shows a similar behavior.

We can show that the maximal value of the peak-to-background ratio for the DD detector approaches 3 when $\Gamma_R, U \gg \gamma, \Omega$ (the dependence on Γ_L is not essential). The same maximal value was obtained for the SET detector [12]. Therefore, while both detectors are sensitive measurement devices, they do not reach the effectiveness of an ideal detector [18].

In summary, we have proposed the use of a double-dot structure for the measurement of a charge qubit. We obtained a set of rate equations describing the entire system and displayed the conditions under which such a measurement is effective. We found the measurement to be most sensitive when the detector operates mainly in the states where no interaction with the qubit takes place. We further demonstrated that, because of quantum interference effects inside the detector, the stationary current is not determined solely by the probabilities of the stationary qubit, but reflects the qubit phase as well.

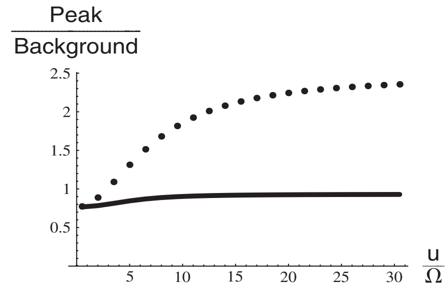

FIG. 4. The peak-to-background ratio of the current power spectrum as a function U for $\Gamma_L = 5\ \Omega$, $\Gamma_R = 10\ \Omega$, and $\gamma = \Omega$. Solid line: qubit positioned next to the detector's left dot, dotted line: qubit positioned next to the detector's right dot.

[1] M. H. Devoret and R. J. Schoelkopf, Nature (London) **406**, 1039 (2000).

[2] D. Mozyrsky, I. Martin, and M. B. Hastings, Phys. Rev. Lett. **92**, 018303 (2004).

[3] W. Lu, Z. Ji, L. Pfeifer, K. W. West, and A. J. Rimberg, Nature (London) **423**, 422 (2003).

[4] D. Sprinzak, E. Buks, M. Heiblum, and H. Shtrikman, Phys. Rev. Lett. **84**, 5820 (2000).

[5] In fact, the use of a double-dot as a sensitive charge detector has attracted considerable attention in recent theoretical and experimental investigations [6,7].

[6] T. Tanamoto and X. Hu, Phys. Rev. B **69**, 115301 (2004); T. Geszti and J. Z. Bernád, Phys. Rev. B **73**, 235343 (2006), and references therein.

[7] R. Brenner, T. M. Buehler, and D. J. Reily, J. Appl. Phys. **97**, 034501 (2005).

[8] J. Yang *et al.*, Nature (London) **422**, 415 (2003).

[9] A similarity of the DD detector with interferometer is more pronounced if we diagonalize the DD system, reducing it to a single dot with two levels carrying the current, S. A. Gurvitz, IEEE Trans. Nanotechnol. **4**, 45 (2005).

[10] S. A. Gurvitz and Ya. S. Prager, Phys. Rev. B **53**, 15 932 (1996).

[11] S. A. Gurvitz, Phys. Rev. B **57**, 6602 (1998).

[12] S. A. Gurvitz and G. P. Berman, Phys. Rev. B **72**, 073303 (2005).

[13] D. K. C. MacDonald, Rep. Prog. Phys. **12**, 56 (1949).

[14] D. Mozyrsky, L. Fedichkin, S. A. Gurvitz, and G. P. Berman, Phys. Rev. B **66**, 161313(R) (2002).

[15] In general, the noise spectrum of the circuit current is given by $\alpha S_L(\omega) + \beta S_R(\omega) - \alpha\beta\omega^2 S_Q(\omega)$ [14], where the coefficients α, β with $\alpha + \beta = 1$ depend on the junction capacities, $S_{L,R}(\omega)$ are the noise spectrum in the leads, and $S_Q(\omega)$ is the charge correlation functions of the DD. In this Letter we take $\beta = 1$ for the definiteness.

[16] This condition for instance, is satisfied for an ideal point-contact detector [17,18]. See also [12].

[17] S. A. Gurvitz, Phys. Rev. B **56**, 15 215 (1997).

[18] A. N. Korotkov, Phys. Rev. B **63**, 085312 (2001).

[19] V. B. Braginsky and F. Ya. Khalili, *Quantum Measurement* (Cambridge University Press, Cambridge, England, 1992).

[20] S. A. Gurvitz, Phys. Lett. A **311**, 292 (2003).